Case Studies in Construction Materials 18 (2023) e02129

Contents lists available at ScienceDirect

Case Studies in Construction Materials

journal homepage: www.elsevier.com/locate/cscm

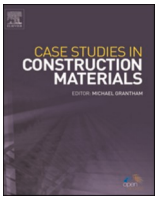

Case study

Modelling of layers interactions on the structural behaviour of insulating glasses. Vertical deflection analyses

Enrico Zacchei [a,c,*], Nuno Simões [b,c], Antonio Vieira [c], Miguel Esteves [a,c], Helder Silva [d]

[a] University of Coimbra, CERIS, Coimbra, Portugal
[b] University of Coimbra, CERIS, Department of Civil Engineering, Coimbra, Portugal
[c] Itecons, Coimbra, Portugal
[d] Silva & Ventura Lda, Company, Rua da Zona Industrial 484, 3740-176 Rocas do Vouga, Portugal

ARTICLE INFO

Keywords:
Insulating glass
Wind actions
Linear loadings
Experimental tests
Numerical analyses
Analytical analyses

ABSTRACT

Insulating glasses (IGs) are composed by glass plates entrapping a cavity filled with a gas sealed by perimeter spacers. This composition pretends to guarantee higher energy efficiency and airborne sound insulation in buildings. The structural performances achieved by these IGs is not normally considered in detail. In fact, in codes there is no specific mechanical model for structural IGs under different loadings and boundary conditions, namely to estimate the vertical deflections when applied horizontally. For this, here a specific model, by combining some existing approaches, was proposed for two or four side supported IG under distributed/linear loadings. The main goal is to quantify if an IG follows a monolith or layered behaviour. Several analytical and numerical analyses using a finite element method (FEM) have been carried out. Then, the results have been validated against experimental laboratory measurements. Two specific IGs with different sizes have been used as case studies. Results show that FEM analyses of IGs are in close agreement with experimental measurements, whereas analytical code models are not as accurate as the numerical approach, in particular for two side supported IGs under linear loadings. Also, the effects of the gas and the interactions between superior and bottom glasses for a large IG are more relevant than for a small IG.

1. Introduction

Insulating glasses (IGs) or insulating glass units (IGUs) are composed by glass plates entrapping a cavity filled with a gas (e.g., air, argon, krypton, xenon [1,2]) sealed by perimeter spacers. Also, aerogels [2] and phase change materials [3] can be applied inside the cavity.

The function of the glass plates is to withstand the external loadings (e.g., wind, snow) as shown in [4] but also external blasts or impacts [5–7], whereas the function of the gas is mainly correlated to a possible reduction of the heat transmittance [2,8–10] or airborne sound insolation [11,12]. Thus, IGs are used to reduce energy consumptions in buildings and to reduce indoor noise level [2].

Due to the brittle nature of the glass, the safety requirements are necessary to use glass structural solutions in building structures as treated in [13], e.g., for transparent roofs, façade, doors, skylights [14–16]. In [17,18] it was highlighted that the glass failure heavily

* Corresponding author at: University of Coimbra, CERIS, Coimbra, Portugal.
E-mail address: enricozacchei@gmail.com (E. Zacchei).

https://doi.org/10.1016/j.cscm.2023.e02129
Received 21 February 2023; Received in revised form 2 May 2023; Accepted 7 May 2023
Available online 9 May 2023

depends on the distribution of flaws on the surface, which are difficult to predict.

In [19] it is noted that the term "structural glass" can lead to misunderstandings since it can refer to point-fixed glazing systems or to glass for structural applications as beam or column elements. In many cases, a structural glass is combined with other materials, e.g., timber [19], steel [20], or "hybrid" glass where there are polymer interlayers, e.g., polyvinyl butyral (PVB) [21], ethylene vinyl acetate, sentry glass plus [22], between different glass layers [23], usually denoted to as "laminated glass".

In accordance with the codes [24,25], IGs can be modelled by two basic approaches [26,27]: (i) independent layered model, where the glass layers are considered independent each other and there is no connection between the glass and the interlayers, being possible free-sliding between them [23]; or (ii) monolithic model, where the structural glasses work as a unique monolithic structure, in which a perfect adherence between all layers allows the transmission of the internal stresses.

However, these approaches could poorly model a structural IG neglecting the presence of the gas [2] and perimeter spacers [20, 28–30].

Many authors have focused their studies on simple models mainly for layered glasses by studying the flexural and torsional behaviour [31], the mechanical performance in terms of bending and shear stresses after and post-racks [22], the influence of the glass type/size [20], the linear pre-crack behaviour considering with pre-stressed cables [32]. Also, in [33] it is studied the positive effects of the plastic deformability of the interlayer in absorbing blast energy.

For IGs modelling, in literature there is the simple "thickness cubed" method, proposed in [34,35], and similar methods proposed in [25,36]. These models basically consider only the glasses geometry. A more refined model, first proposed by [37], accounts for line and point loads on rectangular IGs. More recently, the more efficient Betti's analytical method (BAM), that can be readily used for double IGs of any size and shape, under various boundary and loading conditions, has been proposed in [1,38,39].

To the best of the authors' knowledge, there are few publications regarding the structural response of IGs as [40], analysing the vibration modes of the gas-glass structure; [28], evaluating its structural behaviour accounting for the perimeter spacers under wind pressures; and [35], estimating the load sharing on the glasses accounting for external and internal temperature variations.

More recently, in [2] it was studied the influence of gas on IGs in terms of density and thickness, and in [29] the mechanical properties of IGs in function of glass and gas thickness.

Also, advanced studies on IG are presented at: [41], where it was numerically evaluated the effect of the load sharing and geometric non-linearity on the thickness determination of rectangular glass panes used in cruise ships; [42], where analytical and numerical models were proposed to estimate deflections and stresses for circular and elliptical IGs; and [43], where buckling performances in compressive and bending have been quantified.

In Web of Science database [44], during the period 2002–2022, from a list of 130 articles dedicated to IGs, only approximately 30 discuss their mechanical behaviour. This is a low number of publications, meaning that the research on this topic can be increased. In fact, in [29] it is stated that IG "is currently widely used while its relevant research is very scarce". In this sense as stated in [2], "further research focused on the insulating glass units and their influence on heat transfer throughout the window" is necessary. Therefore, the motivations of this study are:

1) Codes to model an IG should be improved. Italian [24] and European [25] codes and guidance [45], and some papers (e.g., [46]) only quantify the load sharing in glass layers due to the gas pressure. This model basically accounts for the direct forces transferred by the perimeter spacer without considering the real influence of the gas.

2) A flexural model to estimate a maximum vertical deflection for an IG is not considered in international codes. In fact, in [39] it was stated that European code "covers only simply supported IGs under uniformly-distributed loads" and it "does not provide formulae for deflections".

3) As already mentioned, a very recent BAM model [1] in 2020 year it was introduced, however, although it is very efficient there are no experimental laboratory tests that can definitively consolidate it.

For these reasons, in this paper, IGs have been fully studied by analytical, numerical, and experimental analysis to try to reduce some above-mentioned conceptual gaps. In particular, Section 2.1 describes the mechanical models for monolithic and layered. Section 2.3.2 introduces the proposed approach for IGs. In Section 3, five analytical models are developed, as well two numerical analyses by finite element method (FEM); finally, two experimental laboratory measurements are used to validate the analytical and FEM results.

2. Mechanical models

The mechanical modelling for structural glasses can be carried out by using two basic models [24,26], i.e., independent layered or monolithic glass. In this study, an IG composed by three glass plates where the "superior interlayer" is formed by gases of height h_g

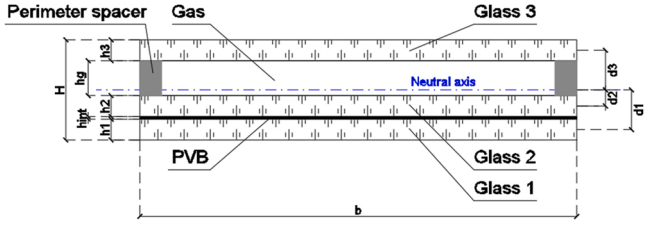

Fig. 1. Cross-section of an IG with three-layers of glass (i.e., inferior laminated glass + gas + superior single glass) [47].

sealed by a perimeter spacer, and the inferior interlayer between two glass plates is a PVB (Fig. 1).

This configuration does not strictly follow neither layered nor monolithic model, therefore it should be necessary to modify these two conventional models to analyse an IG. In Italian code [24] it is indicated that both approaches are valid, however, they could not well model a structural IG.

The independent layered and monolithic model can be adopted when the whole structure is formed by layers of glass of height h_i, and polymer interlayers of height h_{int} with a viscoelastic behaviour [22]. Therefore, by considering the cross-section of a IG with three-layers of glass with a total height H, shown in Fig. 1, both models could be adopted for an IG only if $h_g \equiv h_{int}$ (other parameters will be defined later). Both models follow the classical beam theory.

The proposed model consists in defining an equivalent heigh that accounts for the modified flexural stiffness of the IG due to the presence of the gas and PVB. This is because the increment of the flexural stiffness correlated to inertia of a glass with respect the neutral axis is not totally transferred through the gas. The adopted general concept is that the applied load goes towards the stiffer elements thus being correlated to a further modified stiffness partition.

2.1. Basic models

2.1.1. Layered glass

In this approach the glass layers are considered independent to each other and in the laminated glass there is no connection between the glasses and the interlayer. In this case the transition of stresses is not allowed, and the contribution of the interlayers can be neglected since $E_g >> E_p$, where E_g and E_p is the elastic modulus of the glass and interlayer, respectively (see Section 3) [27,31]. Therefore, the flexural stiffness, E_gI_g, of the whole cross-section is calculated as the sum of the contribution of each layer with respect their centroidal axes by [24]:

$$E_gI_g = E_g \sum_{i=1}^{n} \frac{bh_i^3}{12} \tag{1}$$

where I_g is the inertia moment of the glass, h_i is the i-th layer height (here $n = 3$), and b is the layer width (see Fig. 1).

2.1.2. Monolithic glass

In this approach the glass layers work as a monolithic structure, therefore there is a perfect adherence between all layers, and the stresses transmission is established by a "shear transfer coefficient" as indicated in [25,34,48]. Thus, the flexural stiffness, E_gI_g, accounts for Eq. (1) plus the contribution of the layers and interlayers, E_gI_s, with respect the neutral axis (blue line in Fig. 1) as:

$$E_gI = (E_gI_g) + (E_gI_s) = (E_gI_g) + E_g \sum_{i=1}^{n} (bh_i)d_i^2 \tag{2}$$

where d_i is the distance between the centroidal axis of the i-th layer and the neutral axis of the whole structure.

2.2. Literature models for three-layered structural glass

The structural glass treated in this study is formed by three layers of glasses (i.e., inferior laminated glass + air cavity + superior single glass) (Fig. 1). Thus, two consolidated approaches applied for three-layered glasses are explained below. These approaches were correlate to each other, and they would introduce the proposed model for IGs (Section 2.3.2).

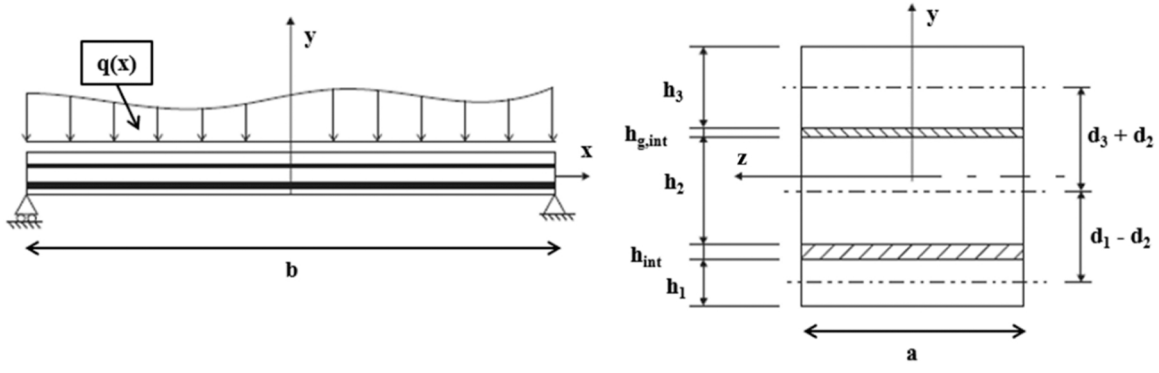

Fig. 2. Cross-section of a three-layered laminated glass.
Modified from [50].

2.2.1. Enhanced effective-thickness approach (Galuppi and Royer-Carfagni, 2012 [49])

The enhanced effective-thickness (EET) approach for laminated glass is an efficient method that allow to solve in a practical way the problems regarding the resistance and deformation of glass structures. This method, defined for glass beams, has been introduced in [49] and extended for glass plates in [4,50]. Fig. 2 shows the mechanical scheme.

This approach assumes that for monolithic limit (i.e., layered model + interlayers contributions) the shear modulus of the interlayer, G, tend to infinity, whereas for the layered limit G tends to 0, as shown in the following Eq. (3). According to the ordinary bending theory, the equilibrium of the forces is described by [49]:

$$\begin{cases} \left(E_g I\right) w'''(x) + q(x) = 0 \quad \rightarrow w(x) \equiv -\dfrac{\widetilde{q}(x)}{E_g I} & \text{Monolithic model}(G\rightarrow\infty) \\ \left(E_g I_g\right) w'''(x) + q(x) = 0 \quad \rightarrow w(x) \equiv -\dfrac{\widetilde{q}(x)}{E_g I_g} & \text{Layered model}(G\rightarrow 0) \\ \left(E_g I_s\right) w'''(x) + q(x) = 0 \quad \rightarrow w(x) \equiv -\dfrac{\widetilde{q}(x)}{E_g I_s} & \text{Layer} - \text{interlayer contributions} \end{cases} \tag{3}$$

where w is the pure bending vertical deflection, the superscript (') indicates differentiation with respect to space x, q(x) is the external load applied to the section as shown in Fig. 2 and $\widetilde{q}(x)$ is a function that is uniquely determined from the form of q(x) and the geometric boundary conditions of the beam.

Therefore, the general solution of Eq. (3) in a unique form can be described by:

$$w(x) \equiv -\frac{\widetilde{q}(x)}{E_g I_R} \tag{4}$$

whit I_R that is an equivalent reduced moment of inertia defined by:

$$\frac{1}{I_R} = \frac{\eta}{I} + \frac{1-\eta}{I_g} \tag{5}$$

where η is a non-dimensional coefficient that accounts for the level of interaction between the glass layers and the interlayers.

The coefficient η depends on the geometry of the beam, its boundary conditions and loading conditions (in [24,51] η was defined by specific relations). For monolithic model $\eta = 1$ (i.e., $I_R = I$), whereas for layered model $\eta = 0$ (i.e., $I_R = I_g$).

One goal of this study is to quantify a value of η, ranging between 0 and 1.0 (i.e., $0 \leq \eta \leq 1.0$), for IGs to estimate the combined real contributions of the PVB interlayer and the gas on the whole IG structure.

Given that w(x) is proportional to I_R (Eq. (4)) thus to the cubed of the thickness i.e., h_i^3, the EET provides a deflection-effective thickness, $\hat{h}_w$, to estimate w(x). From Eq. (5), in an analogue way for a three-layered glass, $\hat{h}_w$ is defined as [4,49]:

$$\left(\frac{1}{\widehat{h}_w}\right)^3 = \frac{\eta}{\sum_{i=1}^{3} h_i^3 + 12\sum_{i=1}^{3} h_i d_i^2} + \frac{(1-\eta)}{\sum_{i=1}^{3} h_i^3} \rightarrow \widehat{h}_w = \sqrt[3]{\left(\frac{\eta}{\sum_{i=1}^{3} h_i^3 + 12\sum_{i=1}^{3} h_i d_i^2} + \frac{(1-\eta)}{\sum_{i=1}^{3} h_i^3}\right)^{-1}} \tag{6}$$

which is valid with two viscoelastic inter-layers h_{int} and $h_{g,int}$ (Fig. 2).

Eq. (6) substantially transforms a three-layer glass in an equivalent monolithic glass; in this sense, the vertical deflection, w, regards the pure bending case whit $G \rightarrow \infty$ as shown also in [31].

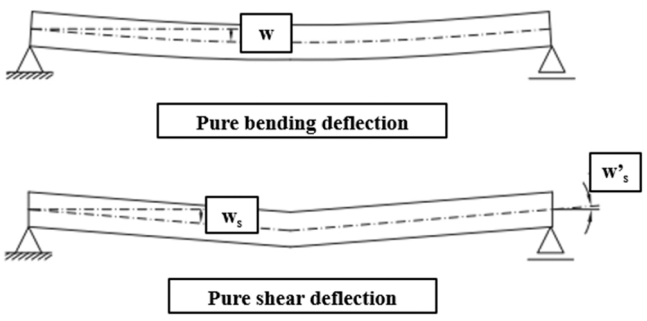

Fig. 3. Pure bending and shear deflection for laminated glass beams.
Modified from [31].

2.2.2. Equivalent flexural model (Machado-e-Costa et al., 2016 [31])

In [31] the cases of multi-layers laminated glasses (from 2 to 5) have been studied. In particular, the case of the three-layered glasses has been considered where the total vertical deflection $w_t(x)$ accounts for the pure bending deflection w(x), already defined in Eq. (4), and the pure shear deflection $w_s(x)$ as shown in Fig. 3; the associated shear forces are V_t, V and V_s, respectively.

The used scheme in this approach (Fig. 3) is like Fig. 2 but considering a concentrated load applied at the middle of the beam (i.e., $V_t(x) = V(x) + V_s(x) \equiv q(x) \times b/2$). The shear deflection w_s can be divided in two components: transverse shear and warping shear deflection (here neglected since the loading is considered symmetric).

Given that contribution of the interlayer for the flexural stiffness is small, the shear stress in the interlayer $\tau_{int}(x)$ can be taken constant across its thickness $h_{int} \equiv h_{g,int}$. The shear stress $\tau_{int}(x)$ can be written as:

$$\tau_{int}(x) = \frac{V_t(x)}{b(d_1+d_3)} \tag{7}$$

The shear force V(x) associated with the pure bending (i.e., $V_s = 0$) displacement w(x) can be expressed as:

$$V(x) = b(d_1+d_3)\tau_{int}(x) - \left(E_g I_g\right) w'''(x) \tag{8}$$

Actually, an interlayer has a finite G value (i.e., G ‡ 0), thus $\tau_{int}(x)$ should be also associated to the pure shear displacement w_s by $\gamma_{int}(x) = \tau_{int}(x)/G$. This indicates that the interlayers contribute with their flexural stiffness by V_s on the total shear force V_t. Therefore, the limit condition regarding Eq. (3) is no longer valid and the system passes from G = 0 to G ‡ 0, and $w_s(x)$ plays an important role.

For this, the total shear force $V_t(x)$ in Eq. (8) can be rewritten as:

$$V_t(x) = \left[b(d_1+d_3)\tau_{int}(x) - \left(E_g I_g\right) w'''(x)\right] - \left(E_g I_g\right) w_s'''(x) \tag{9}$$

The slope of w_s (i.e., w_s') can be expressed by:

$$w_s' = \gamma_{int}\frac{2h_{int}}{(d_1+d_3)} \tag{10}$$

thus

$$\tau_{int} = \gamma_{int} G = \frac{(d_1+d_3)}{2h_{int}} G w_s' \tag{11}$$

By substituting Eq. (11) in Eq. (8) it is obtained:

$$V(x) = \left[b(d_1+d_3)\left(\frac{(d_1+d_3)}{2h_{int}} G w_s'\right)\right] - \left(E_g I_g\right) w'''(x) = \left(\frac{b(d_1+d_3)^2}{2h_{int}} G w_s'\right) - \left(E_g I_g\right) w'''(x) \tag{12}$$

Finally, by explicating w_s' form Eq. (12) and considering Eq. (3), which also account for the pure bending contribution of w(x), i.e., V(x) = - (E_g I) w'''(x) with q(x) ≡ V(x), w_s' can be written as:

$$w_s' = \frac{V(x) + \left(E_g I_g\right)}{\frac{b(d_1+d_3)^2}{2h_{int}} G} w'''(x) = \frac{V(x)}{\frac{b(d_1+d_3)^2}{2h_{int}} G} + \frac{\left(E_g I_g\right)}{\frac{b(d_1+d_3)^2}{2h_{int}} G}\left(-\frac{V(x)}{E_g I}\right) = \frac{V(x)}{\frac{b(d_1+d_3)^2}{2h_{int}} G}\left(1 - \frac{E_g I_g}{E_g I}\right) \tag{13}$$

which can be integrated to provide an expression representative of the total deflection w_t:

$$w_t(x) \approx \int_x \frac{V(x)}{\frac{b(d_1+d_3)^2}{2h_{int}} G}\left(1 - \frac{E_g I_g}{E_g I}\right) dx \tag{14}$$

Eq. (13) thus Eq. (14) provide solutions that would combine both approaches [31,49].

2.3. Insulating glass model

As mentioned, a structural IG could be modelled by abovementioned models. The substantially difference regards the presence of the gas between glass layer 2 and 3 thus h_g ‡ h_{int} (Fig. 1). For a structural IG the current approach usually applied (Section 2.4.1) consists only in quantifying the load sharing in glass layers due to the gas pressure [24,25,45,46].

2.3.1. Load sharing

The under-pressure gas model to estimate the load sharing for each glass layer is usually defined for only one air space between two layers [24,46]. To apply this model to the studied three-layered IGs, here it was considered the inferior glass as a unique block formed by (glass 1 + PVB + glass 2), which can be called “inferior glass” (this is possible by using the abovementioned EET approach). Therefore, other glass (i.e., glass 3) is here called “superior glass”.

By considering a uniform distribute load, q, on the external glass surface, the load can be divided in superior glass, q_{sup}, and inferior

glass, q_{inf}. Depending on where q is applied there are some different cases, i.e., when q is applied on superior glass (i.e., superscript s) and when applied on inferior glass (i.e., superscript i), respectively [25,35,45]:

$$\begin{cases} q^{s}_{sup} = q(\delta_{sup} + \varphi\delta_{inf}) \\ q^{s}_{inf} = q(1-\varphi)\delta_{inf} \end{cases} \tag{15}$$

$$\begin{cases} q^{i}_{sup} = q(1-\varphi)\delta_{sup} \\ q^{i}_{inf} = q(\varphi\delta_{sup} + \delta_{inf}) \end{cases} \tag{16}$$

where δ_i is the stiffness partition regarding the i-th glass, and φ is the insulating unit factor defined as, respectively:

$$\begin{cases} \delta_{sup} = \dfrac{h_3^3}{h_3^3 + (h_1 + h_2)^3} \\ \delta_{inf} = \dfrac{(h_1 + h_2)^3}{h_3^3 + (h_1 + h_2)^3} = 1 - \delta_{sup} \end{cases} \tag{17}$$

$$\varphi = \frac{1}{1 + \left(\frac{a}{a^*}\right)^4} \tag{18}$$

where a* is a characteristic width that mainly depends on h_i, a, b, and the Poisson' ratio of the glass, υ.

Eq. (18) probably is calibrated for IG glasses with common dimensions (e.g., a < 2.0 m [4]), therefore it could underestimate the load sharing for large glass layers. For example, by considering the studied IGs (see Section 3), φ_{IG2} is on average greater than 15.0 × φ_{IG1}, for h_g < 50.0 mm, whereas the $\varphi_{IG2}/\varphi_{IG1}$ ratio, thus gas influence, reduces for h_g > 50.0 mm. For IG1, in general, the values of φ are very low. This could indicate that the approach provided by codes [24,25] needs to more studies to be applied to any IG.

2.3.2. *Proposed flexural approach*

In this work, a new approach for modelling IGs is proposed, which should be valid under the following hypotheses:

1. The glass has a linear-elastic brittle behaviour up to the first cracking and it carries both bending and shear stress. The structural glass is homogeneous, and it follows the classical Euler-Bernoulli assumption where the entire section remain plane and no relative slippage occurs between all layers [23,49]. This is possible if a > > h_i, therefore the shear deformations are constrained resulting in a plane strain response [22]. Possible detachments at the contact surfaces are also neglected [26].

2. The PVB interlayer, between the glass 1 and glass 2, has a viscoelastic behaviour and allow the transmission of the loadings. The height of the interlayer is small with respect the glass height; therefore, it does not affect the global flexural stiffness (i.e., h_{int} << h_i; the h_{int}/h_i ratio, in this work, range between 0.063 and 0.126 [20]). It is assumed linear in-plane stress distributions through laminated glass thickness [5] and for small deflections (< 10.0 mm [52]) [27]. Also, it does not change their mechanical properties during dynamic actions and temperature variations as explained in [23,27,53,54]. However, in this paper, for the inferior glass the EET approach has been adopted under the assumptions shown in [4,24,49].

3. The gas layer can be considered as an ideal gas (inviscid and irrotational [40]) to allow an interaction and transmission of forces between the glass layers (see Fig. 4) [24,35]. However, a real gas does not respect these conditions thus it only partially transmits the forces [1]. In fact, the whole transfer of forces is mainly allowed by stiff perimeter spacers. In this paper, the gas can be considered as homogeneous since IG1 is filled by 90.0% of argon, whereas IG2 by 100.0% of air. The gas pressure is considered uniform, and its

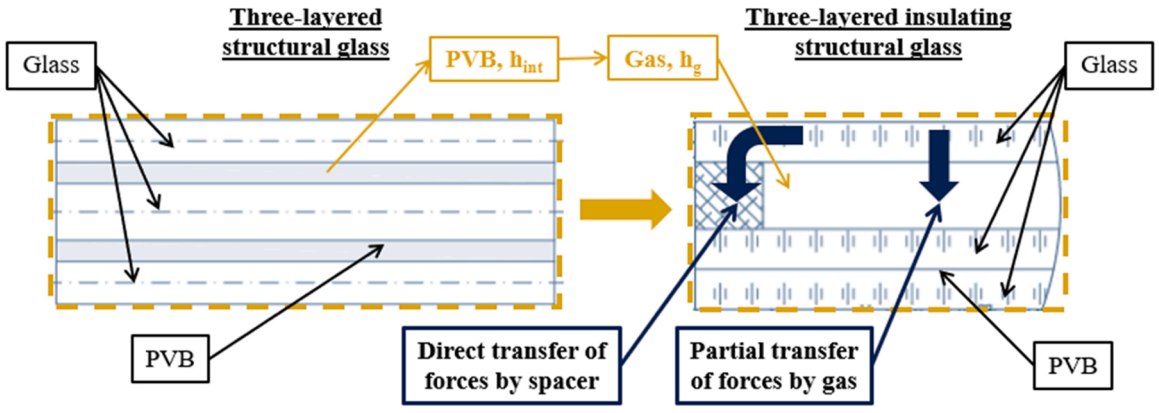

Fig. 4. Conceptualization of the conversion from three-layered laminated glasses to a new three-layered IG (i.e., laminated glass + air cavity + single glass).

variation is small with respect the variation of the external pressures [39]. However, this condition is not always valid since the height h_g can affect this interaction [40].

Therefore, these 3 hypotheses should allow to introduce an equivalent heigh d_i * that accounts for the modified flexural stiffness of the structure due to the presence of the gas. This could be possible by modifying the height d_i in I_s, defined in Eq. (2), by accounting for Eqs. (17)-(18). This is because the increment of the flexural stiffness correlated to I_s is not totally transferred with respect the neutral axis.

The adopted general concept is that the load q goes towards the stiffer elements, therefore it is possible to consider that the uniform distributed load for any combination, i.e., $q^{i/s}_{sup/inf}$, is correlated to a modified stiffness partition, i.e., $q^{i/s}_{sup/inf} \rightarrow d_i{}^* = d_i \times \delta_{sup/inf}$.

In this sense, the adapted relations of Eq. (2) and Eq. (6) are proposed:

$$\begin{cases} E_g \quad I_s^* = E_g \sum_{i=1}^{n} (bh_i)\left(d_i^*\right)^2 \\ \widehat{h}_w^* = \sqrt[3]{\left(\dfrac{\eta}{\sum_{i=1}^{3} h_i^3 + 12\sum_{i=1}^{3} h_i \left(d_i^*\right)^2} + \dfrac{(1-\eta)}{\sum_{i=1}^{3} h_i^3}\right)^{-1}} \end{cases} \tag{19}$$

where η, introduced in Eq. (5), in this paper is estimated a-posteriori and its quantification should represent an innovative aspect.

Eq. (19) indicates that the equivalent system follows a monolithic scheme having the equivalent inertial properties of a real IG since η quantifies the role of the PVB and gas in a unique way on the total elastic deflections w_t.

In literature there are similar approach where a unique equivalent monolithic glass was created [6,26]. In [6] a unique relation (also discussed Section 3.3) to define an "equivalent thickness" for an IG was shown, where substantially the contribution of a whole IG depends on only a single glass + gas (i.e., the interaction between the glasses is neglected). In [26] an equivalent monolithic section has also been created to simulate a three-layered glass. In [55] they are shown American and French codes where a unique equivalent thickness is estimated in function of the stiffness and geometry of each glass.

Fig. 4 shows the conceptualization of the conversion from three-layered structural glass to a new three-layered insulating structural glass (i.e., $h_{int} \rightarrow h_g$).

Fig. 5 shows the trend of the equivalent heigh, $\widehat{h}_w^*$ (Fig. 5a)), and the total deflection, w_t (Fig. 5b)), of the IG in function of the stiffness partition δ_{sup} and δ_{inf} expressed by d_i * in Eq. (19). Both parameters are complementary each other thus when one increases, other parameter decreases. Also, the weight of the η parameters is shown, which, as already mentioned for Eq. (5), defines the tendency of the IG to behave like a monolithic or layered model.

The w_t values were estimated by the relation provided by codes [24,25]: $w_t = k_1 \frac{(a\times b)^2}{\left(\widehat{h}_w^*\right)^3} \frac{q}{E_g}$, where k_1 is a coefficient that depend on geometry and material of the glass, applied loadings, and boundary conditions. The values of k_1 vary from 0.015 to 0.046 as listed in [24,25] (in Fig. 5b), $k_1 = 0.04$). Other parameters have been already explained.

It is important to highlight that w_t follows the Kirchhoff theory for plates [11,38,40], whereas all Section 2.1 was based on Euler-Bernoulli theory for beams. However, Eq. (19) is valid for both theories as stated in [24], and only the η parameter changes, which, in this study, was estimated a-posteriori, therefore the influence of the boundary conditions and geometry are intrinsically considered. In [26] differences between 2D beam and 3D plate model were discussed.

Fig. 6 shows the internal stress σ, strain ε and shear τ diagrams of an IG subjected to a flexural moment M and axial tensile N (in this

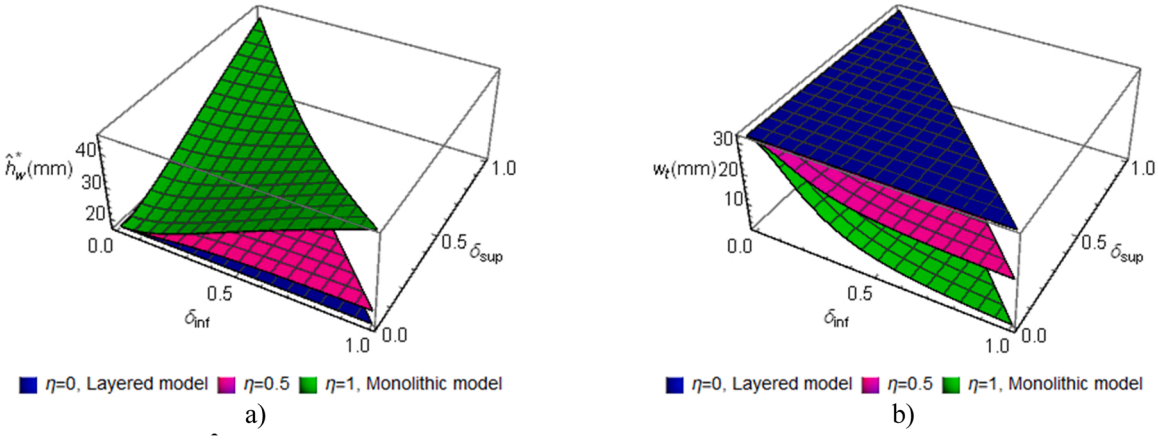

Fig. 5. Trend of a) $\widehat{h}_w^*$ and b) w_t values in function of $\delta_{inf/sup}$ and η (estimated values under q ≈ 2.0 kN/m^2 for IG1).

paper N = 0). By the Navier's relation, stresses σ have been estimated at the indicated points. The trend of the stress and shear diagrams can vary in function of the geometrical parameters and elastic section modulus, W, as shown also in [22] ($W_{g,sup}$ = Elastic section modulus of the superior glass; W_s = Elastic section modulus of the perimeter spacer; W_p = Elastic section modulus of the PVB interlayer; $\widehat{W}_{w,inf}$ = Elastic section modulus regarding the deflection-effective thickness $\widehat{h}_{w,inf}$. The nomenclature for other parameters is equivalent).

The strain diagram maintains a continuous trend due to the constitutive laws. For this diagram, only the parameters are indicated without showing the relation.

Two sections (section A and B) were considered since, as shown in Fig. 4, the transferring of the forces thus stresses follow two different ways. The increasing or decreasing of the σ and τ diagrams is purely indicative as well as all diagram trend, in this sense, this configuration could represent a general case.

As already mentioned, the gas partially transfers the forces thus σ, ε and τ, however a real gas could strongly damp these transferring; therefore, the diagrams in section B at h_g can be considered null. For this reason, N is divided in N_{sup} and N_{inf} like Eq. (15).

3. Experimental, numerical and analytical results

The analyses have been carried out considering a large IG1 and a small IG2. These two different case studies have been selected to try to quantify the influence of the geometry parameters and the cavity thickness h_g. Values of h_g, with a range of 12.0 – 20.0 mm, are usually adopted for IGs as shown in [2]. Both IGs have the same cross-section (see Fig. 1) with the geometrical and mechanical properties shown in Table 1.

Fig. 7 shows the real two prototype provided by Silva & Ventura Lda company, Portugal (https://s-vitech.com/).

3.1. Numerical FEM analyses

Here the numerical modelling by FEMs of both IGs is described.

Both glass and gas are modelled by 3D 8-node solid continuum elements [5]. The glass follows a linear elastic material model (with the E_g and υ shown in Table 1), whereas the gas is a considered as adherent "added mass" to the glass following the Westergaard approach [40].

For the laminated inferior glass, the EET approach has been used in accordance with [4,24,49] to obtain a unique deflection-effective thickness $\widehat{h}_{w,inf}$: for IG1 and IG2, we obtain 21.88 mm (< 25.52 mm) and 6.62 mm (< 8.38 mm), respectively. By neglecting the PVB mass, since for IGI 1.52×10^{-3} m × 9.50 kN/m^3 [20] ≈ 0, the total mass of the bottom two-layered glass corresponds to the two glasses.

These thicknesses estimated by EET method mainly depend on the contribution of each glass plate in terms of flexural stiffness, shear deformation of PVB, loadings and boundary conditions. For this, the η parameter, estimated analytically a-priori, shown in Eq. (5) has been estimated as 0.846 and 0.715 for IG1 and IG2, respectively [50]. Both values indicate that the bottom two-layered glass behave as a monolithic plate glass for an 84.60% (for IG1) and 71.50% (for IG2).

Regarding the gas modelling, the Westergaard approach was used as shown in [40] for IGs, and more in general, in [57–60] for fluid-structure interactions. For this, an equivalent solid mass has been defined where the bulk modulus, k, has been converted in an equivalent elastic modulus, E_{eq}, as $E_{eq} = 3k[1 - (2\upsilon_{eq})]$ [57] where υ_{eq} is the equivalent Poisson's ratio. This relation can assume two limit conditions: (i) fully compressible case (i.e., $\upsilon_{eq} = 0$ thus $E_{eq} = 3k$) where the gas density changes due to pressure variations, thus the effects of the glass deformability are considered [60]; (ii) fully incompressible case (i.e., $\upsilon_{eq} \approx 0.50$, thus $E_{eq} \approx 0$) where the gas pressure variations are null, thus the Westergaard approach is valid and the glass is assumed to be rigid [58,59].

The boundary conditions and the applied external loads are different for the two cases: IG1 is considered as a simple supported plate at all sides under a distributed uniform load of 1.20 kN/m^2 (Section 3.2.1); and IG2 is a simple supported plate only in two minor sides under a concentrate load of 1.741 kN (linearly distributed along the minor side 0.77 m, i.e., 2.26 kN/m) at the plate centre (Section 3.2.2).

In the FEM model the perimeter spacers are considered (~ 20.0 × 20.0 mm for both cases [28]) since the gas volume has been modelled with the real dimensions. In this analysis only the deflections in the middle of the glasses are consider, therefore their influence, studied in other papers [20,26,28–30,43], can be neglected.

Fig. 8 shows the FEM model of the two case studies and their results in terms of vertical deflection carried out by Ansys software [61]. In Fig. 8a) the three solid elements (i.e., top monolithic glass, gas, bottom layered glasses by EET) that constitute the IGs are indicated. IG1 is formed by 576.0 mesh of 250.0 mm and 4461.0 nodes, whereas IG2 is formed by 513.0 mesh of 80.0 mm and 4010.0 nodes. The registered maximum vertical deflection is 4.72 mm and 11.61 mm for IG1 and IG2, respectively, as shown in Fig. 8b).

3.2. Experimental laboratory tests

Two experimental tests have been carried out in the laboratory facilities of Itecons institute, Portugal (https://www.itecons.uc.pt/). The goal of both tests was to measure the maximum vertical deflections of the structural glass. In particular, IG1 was tested under distributed wind actions, whereas IG2 was tested under liner loadings.

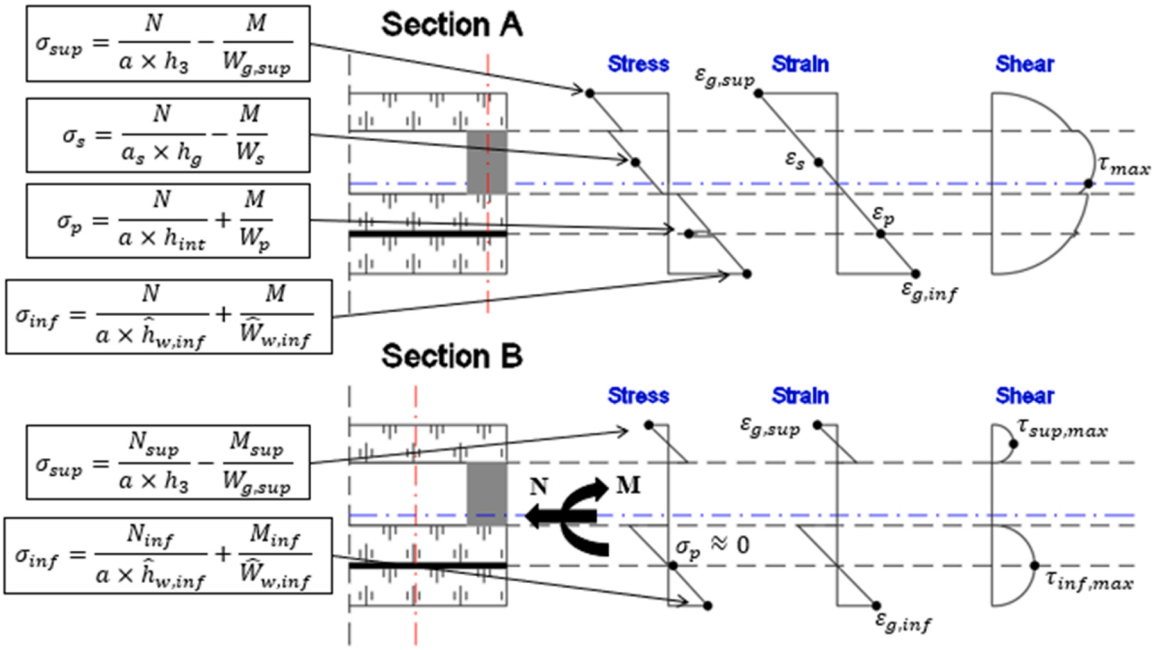

Fig. 6. Stress, strain, and shear diagrams for an IG (general configuration) [47].

Table 1
Geometrical and mechanical parameters (at 20 ºC [27]).

Parameter	Value for IG1	Value for IG2
Glass		
Width, a	3.0 m	0.77 m
Length, b	4.0 m	1.41 m
Layer height, $h_1 = h_2$ [a]	12.0 mm	4.0 mm
Layer height, h_3 [b]	12.0 mm	6.0 mm
Total mass, m	900.0 N/m^2	335.0 N/m^2
Total height, H	57.52 mm	26.38 mm
Elastic modulus, E_g	73.0 GPa[53]	
Poisson's ratio, υ	0.22[2]	
Density, ρ	~25.0 kN/m^3[33]	
PVB interlayer		
PVB height, h_{int} [c]	1.52 mm	0.38 mm
Elastic modulus, E_p	0.30 GPa[20]	
Shear modulus, G	1.50 MPa[22]	
Gas interlayer		
Height gas, h_g	20.0 mm	12.0 mm
Density, ρ_g	1.640 kg/m^3 (90.0% argon)[56] 1.189 kg/m^3 (10.0% air)[56]	1.189 kg/m^3 (100.0% air)[56]

[a] Tempered glass (IG1 = Cool-lite SKN 183 II. IG2 = Sunguard HP neutral 60/40).
[b] Semi-tempered glass (IG1 = Planiclear. IG2 = Colorless laminated).
[c] Standard PVB (4 films for IG1, and 1 film for IG1 of 0.38 mm [5,26]).

3.2.1. Deflections of IG1 under wind loads

The wind test has been carried out in accordance with EN 12211 [62] and EN 12210 [52] codes. Before the testing, the IG1 glass was subjected for ~4.0 h under standard conditions of temperature between 10.0 and 30.0 °C and relative humidity between 25.0% and 75.0%.

For the testing, the IG1 was placed in a test chamber of 5.0 m × 4.0 m, which has sufficient strength and rigidity to withstand the pressures exerted during the tests in accordance with [62].

Fig. 9 shows the IG1 prototype inserted in the test chamber. The function of the superior and inferior metal box is to contain the IG1 glass and to measure the pressures, respectively.

Several positive (+y) and negative (-y) pressures up to 1.20 kN/m^2 were applied on the IG1 where 3 linear variable differential transformers (LVDTs), previously calibrated, measured the vertical deflections of the superior glass (see A, B and C point) as shown in Fig. 10a).

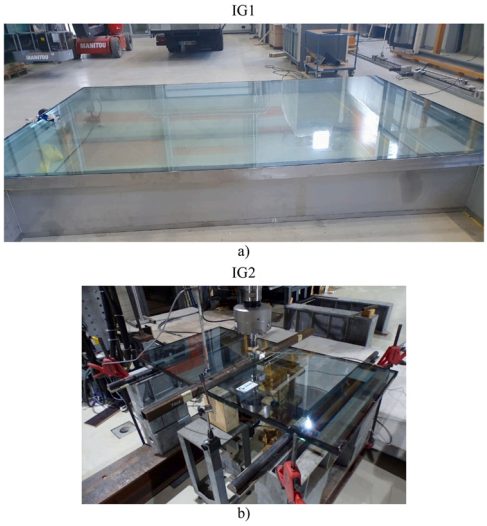

Fig. 7. Analysed prototypes: a) large IG1 and b) small IG2.

Fig. 10b) shows the vertical deflections of the superior glass in function of the wind pressures. As expected, but not obviously due to the spacer stiffnesses as explained in [63], the maximum deflection occurs perfectly in the middle of the glass (i.e., point B) reaching a value of 8.75 mm for 1.20 kN/m^2. In other points the maximum deflection reaches a value of ~1.50 mm.

3.2.2. *Deflections of IG2 under liner loads*

This test was performed by a Instron hydraulic dynamic actuator model DYNSM1745, with a load cell of 50.0 kN from HBK model C2/5 T. Similar to the previous wind test, the vertical deflections were acquired by a LVDT sensor (see point A in Fig. 11a)) from HBK model K-WA in the middle of the glasses (upper and bottom side). The concentrated loads were applied in the point A and then distributed in a central line of 0.77 m. The span between two lateral supports was 1.0 m. The test velocity was 5.0 mm/min of vertical displacement until rupture.

Fig. 11b) shows the vertical deflections for the superior monolithic glass and inferior two-layered glass. The maximum values are 11.18 mm and 9.38 mm for 1.74 kN, then cracks occur. As expected, the two-layered glass has a resistance greater than the monolithic glass of 1.19 (= 11.18/9.38).

3.3. *Discussion of the results*

The results have been plotted by analytic, numerical, and experimental curves to obtain a more complete response for IGs. They are explained as follows:

1) Five analytical results have been plotted, which should provide the exact solutions. These analyses estimate the deflection of the IG glass in a direct way. They are:

- Monolithic superior. It represents the deflection w_t of the only superior glass plate, h_3, under action q distributed by q^s_{sup} defined in Eq. (15) by codes [24,25].
- Layered inferior. It represents the deflection w_t of the two-layered inferior glass, $\widehat{h}_{w,inf}$, under action q distributed by q^s_{inf} defined in Eq. (15) by codes [24,25].
- BAM method. It was proposed in [1,38] to define the deflection w_t of the superior and inferior glass. Currently, it is the most efficient method accounting for the geometry and material characteristics of the glass, loadings, boundary conditions, and internal gas pressures.
- Equivalent monolithic. In [6] it was proposed a unique equivalent thickness of the whole IG (i.e., 0.95 $(h_3^3 + \widehat{h}^3_{w,inf})^{1/3}$). Here it is obtained 21.87 mm and 7.57 mm for IG1 and IG2, respectively.
- Proposed method in the present paper defined by Eq. (19).

2) Numerical FEM results, as explained in Section 3.1.

3) Experimental results (detailed in Section 3.2), which provided more real results since they account for the behaviour of the material, possible imperfections of the glass, load deviations, real geometry, and boundary conditions. These results serve to validate the analytical and FEM results.

Fig. 12 shows the results by using all described models for the IG1 glass. Fig. 12a) shows the vertical deflections trend in function of the applied load (from 0 to 1.20 kN/m^2), whereas Fig. 12b) shows the maximum vertical deflection, $w_{t,max}$ (from 4.72 to 9.50 mm),

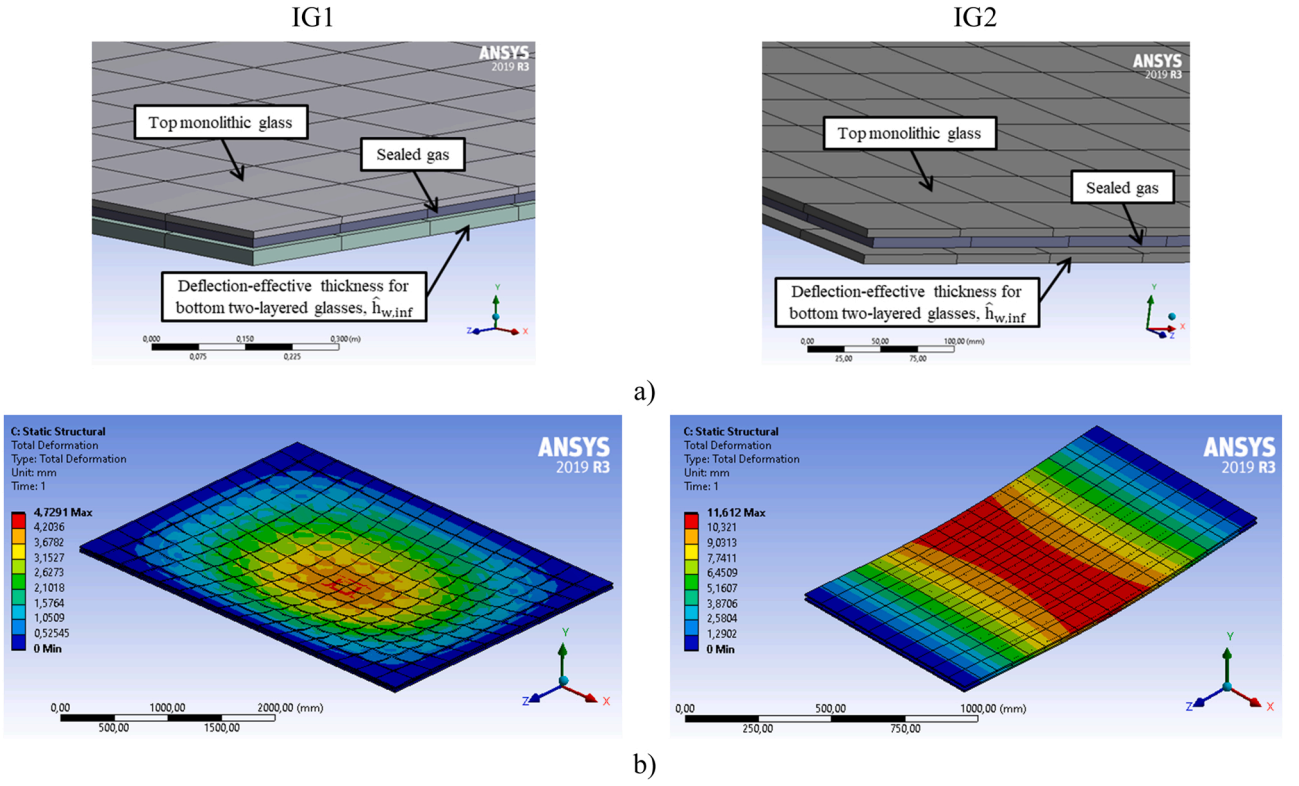

Fig. 8. Numerical analyses by FEM: a) models; b) results.

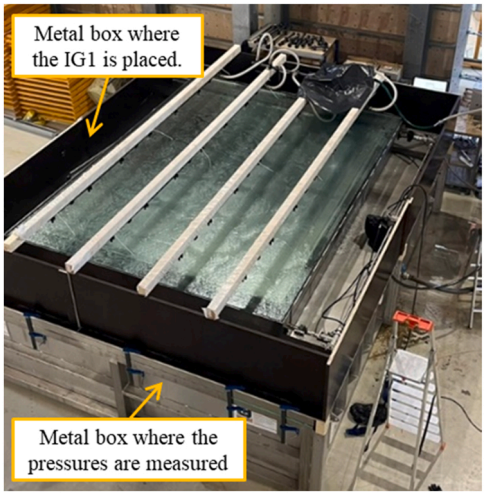

Fig. 9. Prototype inside the test chamber.

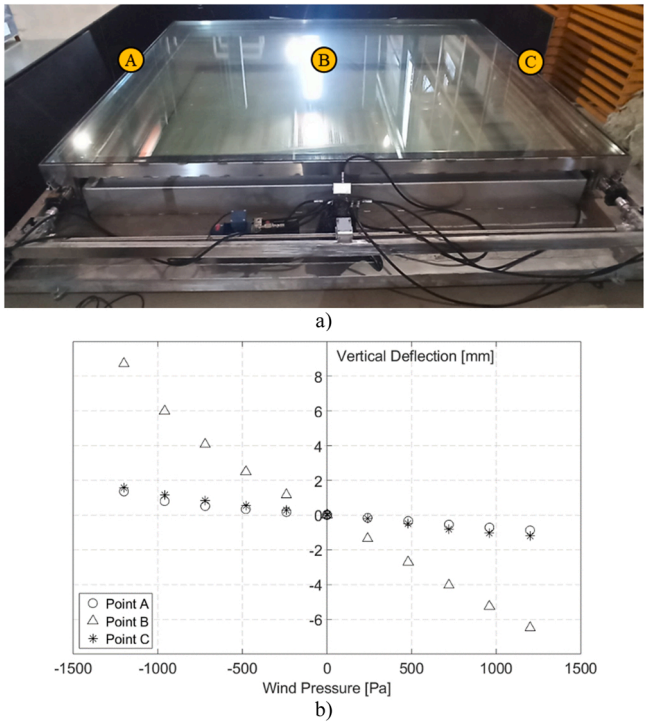

Fig. 10. Wind testing for IG1: a) prototype and LVDT positions; b) results.

and their difference with respect the range (pink band in Fig. 12a)) provided by the proposed model. In this sense, Fig. 12b) should provide the goodness of the estimated η values considering a possible standard deviation ± σ.

The range to estimate η values is included between the BAM and FEM model (dashed lines in Fig. 12a)). This is because for a simple supported IG1 at all sides, under distributed uniform load, both models provide very reliable results as shown in [1,38]. The choice to consider the inferior BAM as upper limit is in favour of the safety and, being a more adequate model, this limit should be in any case considered.

However, as already mentioned, the FEM model is sensible to the gas modelling, which here has been made by the simplify, but efficient, Westergaard approach. Also, BAM model accounts for the gas compressibility (here non considered).

In Fig. 12, results for the layered model provided by codes [24,25] and equivalent monolithic provided by [6] gave high values. The former model refers to the bottom glass therefore strictly is not consistent to the IG1 case since it was measured in the superior glass. In

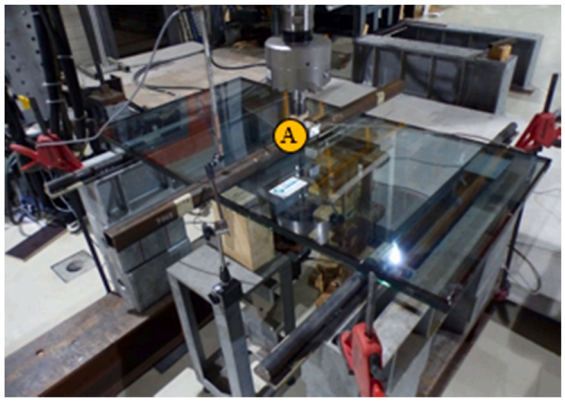

a)

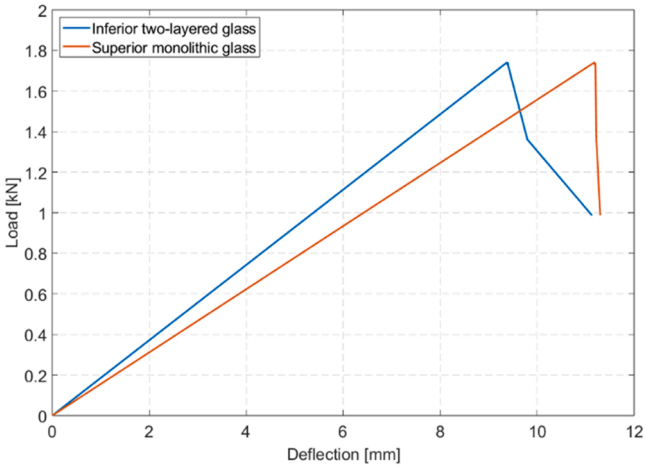

b)

Fig. 11. Linear load testing for IG2: a) prototype and LVDT position; b) load-deflection results.

fact, the difference between layered model and experimental test is 1.94 mm. However, as expected, the layered model represents the upper limit providing the greater deflection as shown in [4,49]. The latter model overestimates the deflection indicating a poor quality of the model; in fact, it is derived based on the assumption of the equal deflection of the upper and lower layers of the insulated glass by quasi-completely neglecting (i.e., 95.0%) the presence of the gas.

Other models show good results since they range between BAM (inferior) and FEM results with a maximum defection difference of 2.51 mm. In Fig. 12b) all differences are highlighted indicating a good agreement of the proposed model for $\eta = 0.74 \pm 0.057$ with BAM (superior), monolithic (superior) and experimental. Experimental results, with respect the other ones, account for the real behaviour of the material.

Another difference among the models, only of IG1, regards the influence of the argon ρ_g, since the models usually are calibrated by air ρ_g. However, this influence can be neglected (here their ratio is 1.37) and in general it is very small as shown in [40].

Fig. 13 shows the results by using all models for the IG2 glass. Here, the range to estimate η values was included between the FEM model and experimental (inferior) (dashed lines in Fig. 13a)). The difference between FEM and experimental (superior) results is 4.0% (in [23,29] it can reach up to ~10.0%).

IG2 is simple supported in two minor sides under a liner load, therefore the BAM model, rigorously, could not be applied; for this reason, in this case, it has not been considered as a valid limit (note that the results from BAM have been amplified of 5.0 by authors to allow some general comparisons [1]).

Differently to IG1, for IG2 the deflections w_t have been obtained by using $k_1 = 0.148$ [24,25] (introduced for Fig. 5) since the boundary conditions are different. Notice that $k_1 = 0.148$ corresponds to a simple 2-side supported rectangular plate under a uniform loading, thus different to this case. Currently, an analytical solution for simple 2-side supported IG under a linear loading do not exist,

[1] From code [24], and in general from classical mechanical theories, it is possible to consider an amplification of 5.0 between a vertical deflection under a uniform loading for 4-side and for 2-side supported glass plate. This value is used only to plot BAM results in Fig. 13, which, for this case, would not represent reliable results.

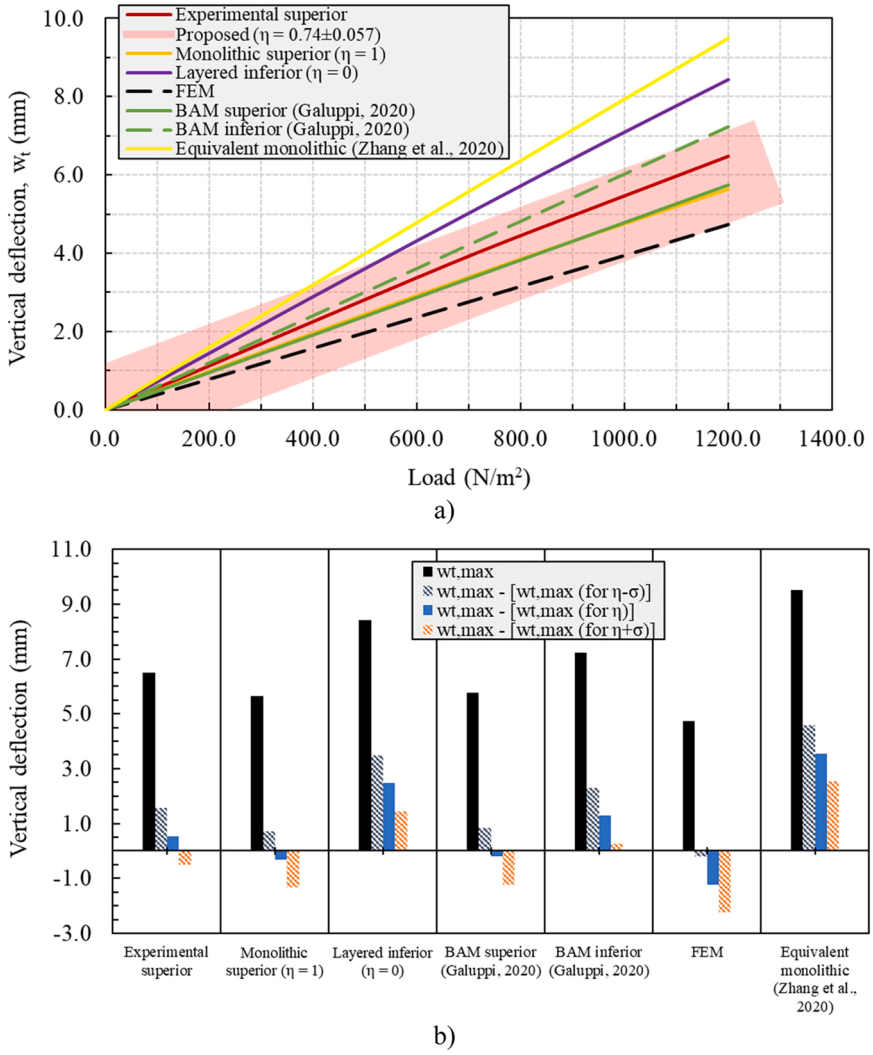

Fig. 12. Results for IG1: a) vertical deflection vs. applied loadings; b) differences between models with respect the proposed model.

therefore here an equivalent q value has been used ($q = 1.741/(0.77 \times 1.41) = 1.60$ kN/m^2). For this reason, in this case there are many results that are distant to the experimental results and the proposed result produces a narrower band.

As for IG1 results (Fig. 12a)), also for IG2 layered and equivalent monolithic model overestimate the vertical deflections. In particular, the layered model is 23.93 mm higher than the experimental (inferior) result, clearly indicating that the model present in the codes [24,25] are not adequate to estimate the behaviour of IGs for linear loadings.

The monolithic model in this case poor estimates the vertical deflection; this is probably due to the fact that load sharing mechanism works bad amplifying δ_{sup} (Eq. (17)) thus q^s_{sup} (Eq. (15)). The difference between both experimental results is not very large since the "participating" hight is similar, i.e., $h_3 \approx \widehat{h}_{w,inf}$.

In Fig. 13b) all differences are highlighted indicating a good agreement of the proposed model for $\eta = 0.88 \pm 0.012$ with FEM and experimental results.

From the obtained η results, it is possible to affirm that the global behaviour of the IG1 is 74.0% monolithic, therefore the partially behaviour of its bottom layered glass (84.60% monolithic estimated in Section 3.1) could be overestimated by considering the contribution of the gas and the superior glass (i.e., 84.60% → 74.0%). For IG2 this percentage becomes 71.50% → 88.0%. In general, this could indicate that the effect of the gas and the superior-inferior glass interactions is more unfavourable for a large IG providing more high vertical deflections.

Finally, Table 2 shows a comparison of the results in the present paper with some studies published in literature. Due to the lack of results in terms of vertical deflections for IGs, two similar studies for layered glasses have been also considered. A good ratio, which would represent the IG linear stiffness, could range between 0.14 and 0.19 indicating, as expected, a high resistance for layered glasses and an overestimation for other cases.

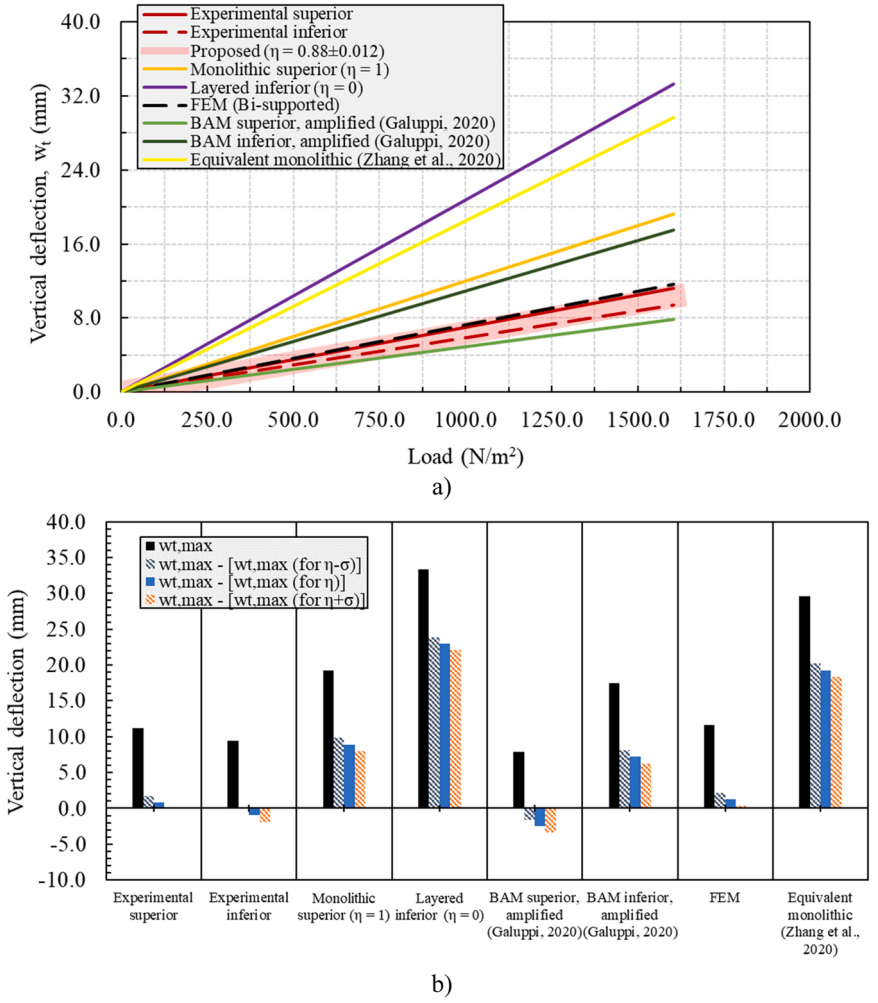

Fig. 13. Results for IG2: a) vertical deflection vs. applied loadings; b) differences between models with respect the proposed model.

Table 2
Comparison with the literature.

Study	a/b	h_g (mm)	h_i (mm)	Load (kN/m^2)	Deflection (mm)	Ratio[a]
Insulating glasses						
Zhang et al. (2021)[29]	0.55	9.0	4.0	3.0	10.55	0.28
Galuppi and Royer-Carfagni (2020)[39]	0.65	12.0	10.0	1.0	4.0	0.25
Galuppi (2020)[1]	0.65	16.0	10.0	1.0	7.0	0.14
Heiskari et al. (2022)[41]	1.0	20.0	10.0	5.0	10.0	0.50
Respondek et al. (2022)[42]	1.0	16.0	4.0	0.09	0.99	0.10
Mean	**0.77**	**14.60**	**7.60**	**2.08**	**6.51**	**0.25**
IG1 (This study)	0.75	20.0	12.0	1.20	6.48 (Fig. 10b))	0.19
IG2 (This study)	0.55	12.0	4.0	1.60	9.38 (Fig. 11b))	0.17
Layered glasses						
Overend et al. (2014)[22]	0.33	N/A[b]	6.0	3.70	10.0	0.37
van Duser et al. (1999)[27]	1.0	N/A	9.52	2.0	7.50	0.27
Mean	**0.67**	-	**7.76**	**2.85**	**8.75**	**0.32**

[a] It would represent the IG linear stiffness calculated as: Load/deflection.[b]Not available (N/A) since it refers to a layered glass.

4. Conclusions

In this paper the vertical deflections for 2 and 4 side supported IGs under uniform and linear loadings have been studied. Analytical, numerical, and experimental analyses have been carried out to provide more complete results. Two specific IGs (a large IG1 and a small

IG2) have been used as case studies.

The main conclusions are:

1) Combining the existing EET approach [49] with the stiffness partition model provided by codes [24,25], a new model is proposed to estimate the mechanical behaviour for IGs. The concept consists in reducing the distance between the centroidal axis of the i-th layer, d_i, by considering the role of the PVB and gas in a unique way on the total elastic deflection. The proposed model follows a monolithic scheme having the equivalent inertial properties of a real IG with a parameter η estimated a-posteriori. The isolated quantification of PVB and gas represents a limit of this model, also it could be difficult to use it a-priori. In this sense, this study represents a qualitative analysis of the mechanical behaviour for IGs.

2) Nine analyses (five analytical, two numerical and two experimental) have been carried out. For both IGs, FEM analyses provide good results, whereas BAM model is valid only for 4-side supported IG1 under uniform loadings. In general, layer and equivalent monolithic models overestimate the vertical deflections. Actually, the former model represents the upper limit providing usually the greater deflection, whereas the latter assumes the equal deflection of the upper and lower layers by quasi-completely neglecting (i.e., 95.0%) the presence of the gas. For two side supported IG2 under linear loadings, it was clear that codes are inadequate.

3) Results show that the bottom two-layered glass of IG1, with a monolithic behaviour of 84.60%, reduces its monolithic behaviour up to 74.0% accounting for the contribution of the gas and the superior glass. IG2 case passes from 71.50% to 88.0%. In general, this could indicate that the effects of the gas and the interactions between superior and bottom glasses for a large IG are more relevant.

Future work can be focused on the experimental validation of the modern BAM model and must provide further analytical solutions for different boundary and loadings conditions, as well in order to understand the real role of the spacers.

Declaration of Competing Interest

The authors declare that they have no known competing financial interests or personal relationships that could have appeared to influence the work reported in this paper.

Data Availability

Data will be made available on request.

Acknowledgements

This work was first carried out under CENTRO-01–0247-FEDER-033896 (S&V SunRoof), funded by Portugal 2020 through COMPETE 2020. The work is now being carried out within the framework of Research Project “R2UTechnologies – Modular Systems” No. C644876810–00000019, investment project No. 48, from the Incentive System to Mobilising Agendas for Business Innovation, funded by the Recovery and Resilience Plan and by European Funds NextGeneration EU.

References

[1] L. Galuppi, Practical expression for the design of DGUs. The BAM approach, Eng. Struct. 221 (2020) 1–21.
[2] K. Banionis, J. Kumziene, A. Burlingis, J. Ramanauskas, V. Paukstys, The changes in thermal transmittance of window insulating glass unites depending on outdoor temperatures in cold climate countries, Energies 14 (2021) 1–22.
[3] C. Liu, Y. Wu, D. Li, Y. Zhou, Z. Wang, X. Liu, Effect of PCM thickness and melting temperature on thermal performance of double glazing units, J. Build. Eng. 11 (2017) 87–95.
[4] L. Galuppi, G. Manara, G. Royer-Carfagni, Practical expression for the design of laminated glass, Compos.: Part B 45 (2013) 1677–1688.
[5] P.A. Hooper, R.A.M. Sukhram, B.R.K. Blackman, J.P. Dear, On the blast resistance of laminated glass, Int. J. Solids Struct. 49 (2012) 899–918.
[6] J. Zhang, X. Wang, L. Wang, P. Su, Experimental study and theoretical verification of explosion-proof performance of insulated glass, Shock Vib. (2020) (2020) 1–6.
[7] X. Zhang, H. Hao, G. Ma, Laboratory test and numerical solution of laminated glass window vulnerability to debris impact, Int. J. Impact Eng. 55 (2013) 49–62.
[8] A.I. Shutov, L.I. Yashurkaeva, S.V. Alekseev, T.V. Yashurkaev, Determination of practical properties of heat-insulating foam glass, Glass Ceram. 65 (2008) 1–5.
[9] A.I. Shutov, L.I. Yashurkaeva, S.V. Alekseev, T.V. Yashurkaev, Modeling of the structure of heat-insulating foam glass, Glass Ceram. 64 (2007) 397–399.
[10] C. Liu, Y. Zhou, D. Li, F. meng, Y. Zheng, X. Liu, Numerical analysis in thermal performance of a PCM-filled double glazing roof, Energy Build. 125 (2016) 267–275.
[11] A. Tadeu, J. Antonio, D. Mateus, Sound insulation provided by single and double panel walls-a comparison of analytical solutions versus experimental results, Appl. Acoust. 65 (2004) 15–29.
[12] A.J.B. Tadeu, D.M.R. Mateus, Sound transmission through single, double and triple glazing, Exp. Eval., Appl. Acoust. 62 (2001) 307–325.
[13] M. Badalassi, L. Biolzi, G. Royer-Carfagni, W. Salvatore, Safety factors for the structural design of glass, Constr. Build. Mater. 55 (2014) 114–127.
[14] L. Figuli, Z. Zvakova, C. Bedon, Design and analysis of blast loaded windows, Procedia Eng. 192 (2017) 177–182.
[15] X. Zhang, H. Hao, Z. Wang, Experimental investigation of monolithic tempered glass fragment characteristics subjected to blast loads, Eng. Struct. 75 (2014) 259–275.
[16] J. Cai, Y. Xu, J. Zhang, Design and analysis of a glass roof structure, Struct. Des. Tall Spec. Build. 22 (2013) 677–686.
[17] J. Wei, L.R. Dharani, Response of laminated architectural glazing subjected to blast loading, Int. J. Impact Eng. 32 (2006) 2032–2047.
[18] X. Zhang, H. Hao, G. Ma, Parametric study of laminated glass window response to blast loads, Eng. Struct. 56 (2013) 1707–1717.
[19] Z. Unuk, I. Lukic, V.Z. Leskovar, M. Premrov, Renovation of timber floors with structural glass: Structural and environmental performance, J. Build. Eng. 38 (2021) 1–11.
[20] C. Louter, J. Belis, F. Veer, J.P. Lebet, Structural response of SG-laminated reinforced glass beams; experimental investigations on the effects of glass type, reinforcement percentage and beam size, Eng. Struct. 36 (2012) 292–301.
[21] L. Biolzi, S. Cattaneo, G. Rosati, Progressive damage and fracture of laminated glass beams, Constr. Build. Mater. 24 (2010) 577–584.
[22] M. Overend, C. Butchart, H. Lambert, M. Prassas, The mechanical performance of laminated hybrid-glass units, Compos. Struct. 110 (2014) 163–173.
[23] M. Lopez-Aenlle, F. Pelayo, Dynamic effective thickness in laminated-glass beams and plates, Compos.: Part B 67 (2014) 332–347.

[24] National Research Council (CNR), Instructions for the Design, Execution and Control of Constructions with Structural Elements of glass, CNR-DT 210/2013, Rome, Italy, p. 362, 2013.
[25] CEN-TC129-WG8, EN-16612: Glass in building – determination of the load resistance of glass panes by calculation and testing. European Standard, 2013.
[26] C. Bedon, C. Louter, Exploratory numerical analysis of SG-laminated reinforced glass beam experiments, Eng. Struct. 75 (2014) 457–468.
[27] A. van Duser, A. Jagota, S.J. Bennison, Analysis of glass/polyvinyl butyral laminates subjected to uniform pressure, J. Eng. Mech. 125 (1999) 435–442.
[28] J.R. Bailey, J.E. Minor, R.W. Tock, Response of structurally glazed insulating glass units to wind pressure, J. Wind Eng. Ind. Aerodyn. 36 (1990) 1163–1171.
[29] X. Zhang, J. Liang, D. Huang, Study on the mechanical response of anticlastic cold bending insulating glass and its coupling effect with uniform load, Plos One 16 (2021) 1–22.
[30] S. Buddenberg, P. Hof, M. Oechsner, Climate loads in insulating glass units: comparison of theory and experimental results, Glass Struct. Eng. 1 (2016) 301–313.
[31] M. Machado-e-Costa, L. Valarinho, N. Silvestre, J.R. Correira, Modeling of the structural behavior of multilayer laminated glass beams: flexural and torsional stiffness and lateral-torsional buckling, Eng. Struct. 128 (2016) 265–282.
[32] S. Jordão, M. Pinho, L.C. Neves, J.P. Martins, A. Santiago, Behaviour of laminated glass beams reinforced with pre-stressed cables, Steel, Construction 7 (2014) 204–207.
[33] H.D. Hidallana-Gamage, D.P. Thambiratnam, N.J. Pereram, Numerical modelling and analysis of the blast performance of laminated glass panels and the influence of material parameters, Eng. Fail. Anal. 45 (2014) 65–84.
[34] ASTM: Standard practice for determining load resistance of glass in buildings, ASTME 1300–12,West Conshohocken, PA, 2012.
[35] S.M. Morse, H.S. Norville, Comparison of methods to determine load sharing of insulating glass units for environmental loads, Glass Struct. Eng. 1 (2016) 315–329.
[36] Siebert G., Maniatis I. Tragende Bauteile aus Glas: Grundlagen, Konstruktion, Bemessung, Beispiele. John Wiley & Sons; 2012.
[37] F. Feldmeier, How to handle climatic loads in the design of insulating glass units [Zur Beruecksichtigung der Klimabelastung bei der Bemessung von Isolierglas bei Ueberkopfverglasung], Stahlbau 65 (8) (1996) 285–290.
[38] L. Galuppi, G. Royer-Carfagni, Betti's analytical method for the load sharing in double glazed units, Compos. Struct. 235 (2020) 1–14.
[39] L. Galuppi, G. Royer-Carfagni, Green's function for the load sharing in multiple insulating glazing units, Int. J. Solids Struct. 206 (2020) 412–425.
[40] W.P. Vann, Y.C. Das, Free vibration analysis of insulating glass units, J. Wind Eng. Ind. Aerodyn. 36 (1990) 1145–1153.
[41] J. Heiskari, J. Romanoff, A. Laakso, J.W. Ringsberg, On the thickness determination of rectangular glass panes in insulating glass units considering the load sharing and geometrically nonlinear bending, Thin-Walled Struct. 171 (2022) 1–13.
[42] Z. Respondek, M. Kozlowski, M. Wisniowski, Deflections and stresses in rectangular, circular and elliptical insulating glass units, Materials 15 (2022) 1–17.
[43] C. Bedon, C. Amadio, Buckling analysis and design proposal for 2-side supported double Insulated Glass Units (IGUs) in compression, Eng. Struct. 168 (2018) 23–34.
[44] Web of Science (WoS), database, accessed on 01/2023. https://www.webofscience.com/wos/.
[45] Joint Research Centre of the European Commission, Guidance for European Structural Design of Glass Components, EUR 26439 EN, p. 208, 2014.
[46] S.M. Mores, H.S. Norville, Comparison of methods to determine load sharing of insulating glass units for environmental loads, Glass Struct. Eng. 1 (2016) 315–329.
[47] AutoCAD, software, version 2010, Autodesk, Inc., 2010.
[48] O.' Regan C, The institution of structural engineers, technical manual, Struct. Use Glass Build., Lond., Engl. (2015) 118.
[49] L. Galuppi, G.F. Royer-Carfagni, Effective thickness of laminated glass beams: new expression via a variational approach, Eng. Struct. 38 (2012) 53–67.
[50] L. Galuppi, G. Royer-Carfagni, The effective thickness of laminated glass plates, J. Mech. Mater. Struct. 7 (2012) 1–29.
[51] Galuppi, L., Royer Carfagni, G., The enhanced effective thickness method for laminated glass, Proceedings Glass Per-formance Days (GPD) 2013, p. 36, Tempere Finland, June 13–15, 2013.
[52] Windows and doors - Resistance to wind load - Classification, EN 12210:2016, Brussels, Belgium, 2016.
[53] M. Botz, M.A. Kraus, G. Siebert, Sensitivity analysis for the determination of the interlayer shear modulus in laminated glass using a torsional test, Glass Struct. Eng. 3 (2018) 355–371.
[54] F. Pelayo, M.J. Lamela-Rey, M. Muniz-Calvante, M. Lopez-Aenlle, A. Alvarez-Vazquez, A. Fernandez-Canteli, Study of the time-temperature-dependent behaviour of PVB: application to laminated glass elements, Thin-Walled Struct. 119 (2017) 324–331.
[55] J. Sanches, Analysis and design of structural glass systems, Higher Technical Institute (IST), Lisbon, Portugal (2013) 1–11.
[56] L. Galuppi, M. Maffeis, G. Royer-Carfagni, Engineered calculation of the uneven in-plane temperatures in Insulating Glass Units for structural design, Glass Struct. Eng. (2022) (2022) 1–29.
[57] Furgani, L.. Verifiche Sismiche di Dighe in Calcestruzzo. Ph.D. Thesis, University of Roma Tre, Rome, Italy, 2014.
[58] E. Zacchei, J.L. Molina, Reviewing arch-dams' building risk reduction through a sustainability-safety management approach, Sustainability 12 (2020) 1–24.
[59] A.T. Chwang, G.W. Housner, Hydrodynamic pressures in sloping dams during earthquakes, Part 1. Momentum Method. J. Fluid Mech. 87 (1978) 335–341.
[60] P. Chakrabarti, A.K. Chopra, Earthquake analysis of gravity dams including hydrodynamic interaction, Earthq. Eng. Struct. Dyn. 2 (1973) 143–160.
[61] Ansys R3 academic, software, 2019.
[62] Windows and doors - Resistance to wind load- Test method, EN 12211:2016, Brussels, Belgium, 2016.
[63] Timoshenko, S., Woinowsky-Krieger, S., Theory of Plates and Shells, McGraw-Hill Book Company Editor, p. 591, 1989.